Dynamic Magnetic Resonance Measurements of Calf Muscle Oxygenation and Energy Metabolism in Peripheral Artery Disease

Adrianus J. Bakermans, PhD,[1]* ● Chang Ho Wessel, MD,[2] Kang H. Zheng, MD,[2]
Paul F.C. Groot, PDEng, MSc,[1] Erik S.G. Stroes, MD, PhD,[2] and Aart J. Nederveen, PhD[1]

Background: Clinical assessments of peripheral artery disease (PAD) severity are insensitive to pathophysiological changes in muscle tissue oxygenation and energy metabolism distal to the affected artery.
Purpose: To quantify the blood oxygenation level-dependent (BOLD) response and phosphocreatine (PCr) recovery kinetics on a clinical MR system during a single exercise-recovery session in PAD patients.
Study Type: Case–control study.
Subjects: Fifteen Fontaine stage II patients, and 18 healthy control subjects
Field Strength/Sequence: Interleaved dynamic multiecho gradient-echo ^{1}H T_2^* mapping and adiabatic pulse-acquire ^{31}P-MR spectroscopy at 3T.
Assessment: Blood pressure in the arms and ankles were measured to determine the ankle-brachial index (ABI). Subjects performed a plantar flexion exercise-recovery protocol. The gastrocnemius and soleus muscle BOLD responses were characterized using the T_2^* maps. High-energy phosphate metabolite concentrations were quantified by fitting the series of ^{31}P-MR spectra. The PCr recovery time constant (τ_{PCr}) was derived as a measure of in vivo mitochondrial oxidative capacity.
Statistical Tests: Comparisons between groups were performed using two-sided Mann–Whitney U-tests. Relations between variables were assessed by Pearson's r correlation coefficients.
Results: The amplitude of the functional hyperemic BOLD response in the gastrocnemius muscle was higher in PAD patients compared with healthy subjects ($-3.8 \pm 1.4\%$ vs. $-1.4 \pm 0.3\%$; $P < 0.001$), and correlated with the ABI ($r = 0.79$; $P < 0.001$). PCr recovery was slower in PAD patients ($\tau_{PCr} = 52.0 \pm 13.5$ vs. 30.3 ± 9.7 sec; $P < 0.0001$), and correlated with the ABI ($r = -0.64$; $P < 0.001$). Moreover, τ_{PCr} correlated with the hyperemic BOLD response in the gastrocnemius muscle ($r = -0.66$; $P < 0.01$).
Data Conclusion: MR readouts of calf muscle tissue oxygenation and high-energy phosphate metabolism were acquired essentially simultaneously during a single exercise-recovery session. A pronounced hypoxia-triggered vasodilation in PAD is associated with a reduced mitochondrial oxidative capacity.
Level of Evidence: 2
Technical Efficacy: Stage 1

PERIPHERAL ARTERY DISEASE (PAD) is characterized by progressive narrowing of the lumen (stenosis) in peripheral arteries, which is caused by atherosclerosis in the vast majority of patients. PAD is highly prevalent, and most often reflects a polyvascular disease state that is associated with very high cardiovascular morbidity and mortality numbers.[1,2] Patients with lower extremity PAD may be asymptomatic, present with atypical leg symptoms, or suffer from intermittent

claudication triggered by exertion of the muscle groups distal to the affected artery.[3] This discomfort or pain, classically following exercise, reflects the insufficient capacity of the affected large artery to meet the increased demand for oxygen-rich blood.

The presence and degree of PAD can most easily be established noninvasively with the ankle-brachial index (ABI), which is the ratio of the systolic blood pressure at the ankle to the systolic blood pressure in the arm.[4] The ABI provides a measure of PAD severity in large arteries, but is not sensitive to any pathophysiological changes in the muscle tissue distal to the affected artery, which is necessary to assess the functional consequences of impaired oxygen delivery due to arterial stenosis.[5] Assessments of skin perfusion, such as transcutaneous oxygen pressure ($TcpO_2$) measurements and laser Doppler flowmetry, offer additional readouts, but only become informative at endstage PAD.[5] In view of the mostly modest improvements that preclude the use of a rather gross measurement scale such as the ABI, techniques that quantify tissue perfusion, oxygenation, or energy metabolism will be instrumental for testing and monitoring of therapeutic interventions in PAD. Noninvasive magnetic resonance (MR) methods can provide such indices.[6,7]

Phosphorus-31 MR spectroscopy (^{31}P-MRS) has been widely used to study in vivo muscle high-energy phosphate metabolism through the direct detection of phosphocreatine (PCr), adenosine 5′-triphosphate (ATP), and inorganic phosphate (P_i). Combined with an exercise protocol, dynamic ^{31}P-MRS offers a window on the PCr recovery kinetics that reflect in vivo mitochondrial oxidative capacity.[8] In PAD patients, ^{31}P-MRS has revealed prolonged PCr recovery time constants in exercise-stressed calf muscle compared with healthy control subjects.[9–12] Those data suggest a metabolic impairment of muscle tissue in PAD, which may be related to reduced oxygen supply. Tissue oxygenation can indirectly be assessed by making use of the blood oxygenation level-dependent (BOLD) contrast mechanism in MRI. BOLD MRI exploits the local increase in the proton (^{1}H) T_2^* relaxation time constant, caused by an increasing inflow of oxygenated blood. A different BOLD response in muscle tissue of PAD patients compared with age-matched control subjects has been demonstrated with BOLD MRI during postocclusive reactive hyperemia[13] or after physical exercise,[14] demonstrating that flow of oxygenated blood into tissue distal to the affected artery can be impaired in PAD.

MR assessments of skeletal muscle (patho)physiology are typically conducted during a dynamic measurement, eg, during exercise-recovery or ischemia-reperfusion paradigms. Current MR practice allows probing of only one contrast mechanism with a particular sequence and limits the number of parameters that can be measured during one experiment. Moreover, clinical MR system constraints usually restrict the examination to only one nucleus per session. Consequently, separate experimental sessions are required to probe multiple aspects of pathophysiology, which is particularly problematic

for dynamic studies.[12,15] Idle time during the long repetition time (TR) typically required for ^{31}P-MRS has been efficiently filled with [1]H-MRI acquisitions in previous work on research MR systems.[16,17] In the current study, we aimed to employ such interleaved acquisitions of quantitative T_2^* maps for the assessment of the BOLD response and ^{31}P-MR spectra for measuring PCr recovery kinetics on a clinical MR system. We hypothesized that both muscle tissue oxygenation as well as energy metabolism are affected in PAD patients compared with healthy subjects, and demonstrated that both readouts could be obtained during a single calf muscle exercise-recovery session.

Materials and Methods
Subjects
This observational case–control study was conducted according to the principles of the Declaration of Helsinki (October 2013). The protocol was approved by the local Ethics Committee (NL52059.018.14; Academic Medical Center, University of Amsterdam, Amsterdam, The Netherlands). All subjects provided written informed consent prior to participation.

Patients (n = 15) of 40 years of age or older, with exertional pain in the lower leg (Fontaine stage II)[18] and ultrasound-confirmed stenosis or occlusion in a proximal artery, were recruited from the outpatient clinic of the Department of Vascular Medicine and Vascular Surgery at the Academic Medical Center in Amsterdam. Healthy subjects (n = 18) of 40 years of age or older with no history of cardiovascular disease were included as a control group. Exclusion criteria for both groups included muscular disease, diabetes mellitus, metabolic disease, and contraindications for MR examination. Body height and weight were measured to determine the body mass index (BMI). Venous blood was collected for a complete blood count, and cholesterol, triglyceride, and glucose assays. Blood pressure in both arms and at both ankles was measured to determine the resting ABI.

MR Protocol
All MR experiments were conducted on a 3T MR system (Ingenia, software R5.1.8; Philips, Best, The Netherlands) equipped with a vendor-supplied ^{31}P-MR surface coil (Ø 140 mm, 51.8 MHz; Philips) for RF transmission and signal reception. For shimming and [1]H-MRI, the whole-body birdcage coil integrated in the MR system was used (Ø 70 cm, 127.8 MHz). Subjects were positioned supine, with the foot of the leg with the lowest resting ABI against the pedal of an in-house-built plantar flexion exercise device affixed to the patient table. This device consisted of an angulated pedal supported by a roller that is guided in recesses to support repetitive movement by plantar flexion with an extended knee. Work load could be increased by adding elastic bands attached to the roller. The ^{31}P-MR surface coil was centered underneath the calf muscle belly and fixed by straps that were loosely wrapped around the lower leg. Correct positioning of the ^{31}P-MR surface coil was confirmed by a coil marker visible on survey scans. Then a single-slice transverse T_1-weighted scan through the calf muscle belly and ^{31}P-MR surface coil center was acquired for muscle group identification and segmentation purposes.

The dynamic scan series consisted of 1) a multiecho gradient-echo sequence for [1]H T_2^* mapping of the BOLD response in the transverse

plane with the following scan parameters: field of view 192 × 192 mm; matrix 64 × 64; slice thickness 10 mm; flip angle 15°; 15 echoes; echo time (TE) 1.11 msec +1.8 msec/step; TR 28 msec; acquisition time/T_2* map 1.8 sec, and 2) a pulse-acquire ^{31}P-MRS acquisition: adiabatic excitation; on-resonance frequency between PCr and γ-ATP; 2048 acquisition points; bandwidth 58 ppm (3000 Hz). The volumes for shimming were set for both scans separately, enclosing the entire calf musculature for T_2* mapping, and the sensitive area of the ^{31}P-MR surface coil for ^{31}P-MRS, respectively. Both scans were triggered by an external trigger signal that was set to 1 Hz. A series of 200 acquisitions for both scans were interleaved,[19] resulting in an effective TR of 3 seconds for both scans (Fig. 1) and a total duration of 10 minutes. First, 20 acquisitions for both scans were obtained under resting conditions (ie, 20 × TR 3 sec = 1 min), after which the subjects were instructed to start plantar flexion exercise by pushing the pedal at a steady rate of 1 repetition per second. The repetitive movement of the calf was synchronized with the MR acquisitions via the trigger signal that was visualized on a screen next to the scanner, displaying a bouncing ball at 1 Hz to guide the subject in maintaining exercise rhythm. Subjects were encouraged to maintain exercising until exhaustion, or until the increasing P_i peak amplitude leveled with the decreasing PCr peak amplitude in the ^{31}P-MR spectrum. Whichever occurred first, this was typically between 1 and 3 minutes of exercise, after which the subject was instructed to cease exercise, remain still and relaxed for the remainder of the dynamic acquisitions during subsequent recovery.

Finally, the transverse T_1-weighted scan was repeated to assess potential displacement of the calf compared with its starting position prior to exercise.

MR Data Analyses

BOLD MRI. Tissue oxygenation dynamics were evaluated through a characterization of the BOLD response in transverse ^{1}H T_2* maps of the calf musculature. These maps were calculated online from the multiecho image series per timepoint using the standard vendor-supplied software (R5.1.8; Philips). Consecutive T_2* maps were registered to the T_1-weighted image acquired after recovery by rigid-body registration of the first-echo image within each multiecho image series using elastix 4.8[20] in MatLab R2014a (MathWorks, Natick, MA). Images acquired during exercise were not included in the analyses due to motion artifacts that compromised the calculation of reliable T_2* maps. Regions of interest (ROI) were defined by the same observer through manual segmentations of the T_1-weighted image, outlining the gastrocnemius and soleus muscles, while carefully excluding major vessels and adipose tissue. Per participant, the median transverse relaxation rate constant R_2* = $1/T_2$* per ROI per timepoint were normalized to the average R_2* per ROI for the last 20 timepoints at end-recovery. The dynamic BOLD response during recovery was then visualized by plotting the normalized R_2* against time. From these curves, we quantified the degree of exercise-induced tissue deoxygenation as the median of the normalized R_2* (%) in the first five timepoints after cessation of plantar

flexion exercise. Tissue hyperemia was defined as a transient increase of tissue oxygenation beyond the noise level: a decrease in R_2* by more than twice the standard deviation (SD) of the R_2* over the last 20 timepoints at end-recovery, and was quantified by the minimum relative value in R_2* (%). The time-to-peak (sec) for hyperemia, if any, was defined as the elapsed time between cessation of exercise and the R_2* minimum.

^{31}P-MRS. Muscle high-energy phosphate metabolism was assessed by a quantitative evaluation of ^{31}P-MR spectra from the calf musculature. Spectra were fitted in the time domain using AMARES in jMRUI.[21] Signals from PCr, γ-ATP (doublet), α-ATP (doublet), β-ATP (triplet), P_i, and phosphodiesters (PDE) were fitted to Lorentzian line shapes. The PCr and PDE line widths for recovery were constrained to their average unconstrained line widths during recovery, excluding the first five data points after the end of exercise. Signal amplitudes were corrected for partial saturation, and used to estimate absolute metabolite concentrations by assuming a tissue ATP concentration of 8.2 mM at rest.[22] Intracellular pH was determined using the chemical shift difference between the P_i and PCr signals.[23] The free cytosolic adenosine diphosphate (ADP) concentration was calculated from the PCr concentration and pH, with a creatine kinase equilibrium constant (K_{eq}) of 1.66 × 10^9 L/mol[24] and assuming that 15% of the total creatine is unphosphorylated (ie, free creatine) at rest[25] according to:

$$[ADP] = [ATP][free\ creatine]/[PCr][H^+]K_{eq}$$

PCr recovery kinetics were modeled by a monoexponential function fitted to the PCr concentration curve after exercise:

$$PCr(t) = PCr_{end-recovery} - \Delta PCr \times \exp(-t/\tau_{PCr})$$

with $PCr_{end-recovery}$ the PCr concentration (mM) after recovery, ΔPCr (%) the difference between the $PCr_{end-recovery}$ and the PCr concentration at the end of exercise, and τ_{PCr} the PCr recovery time constant (sec). Data sets fitted with a coefficient of determination (r^2) less than 0.70 or a PCr depletion of less than 15% were excluded from further analyses.

Statistical Analyses

Data are reported as the mean ± SD. Comparisons between PAD patients and healthy subjects were performed using two-sided Mann–Whitney U-tests for independent samples. Relations between variables were assessed by Pearson's r correlation coefficients. The level of significance was set at $P < 0.05$.

Results

Fifteen PAD patients and 18 healthy subjects were recruited for an exercise-recovery protocol of the calf muscle during interleaved acquisitions of T_2* maps and ^{31}P-MR spectra.
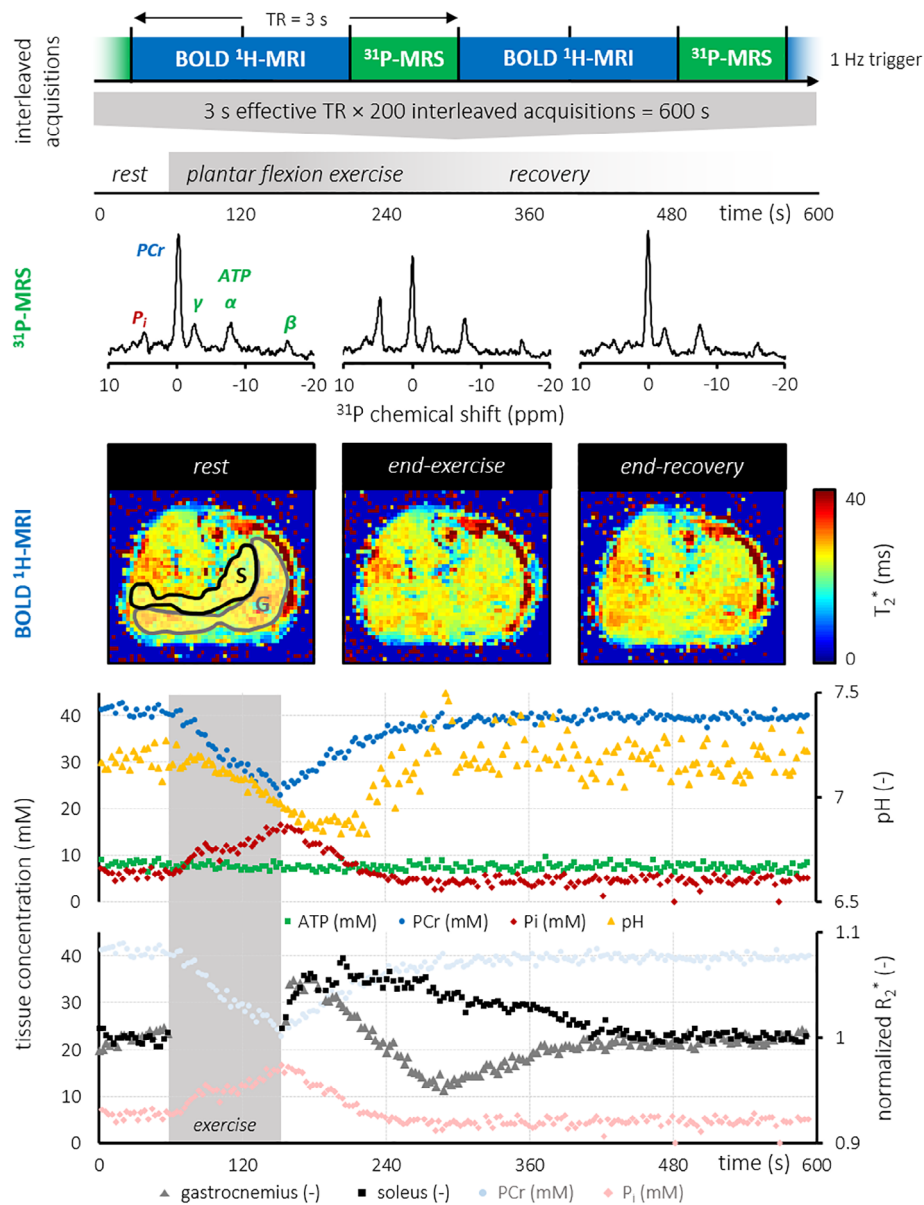
FIGURE 1: Overview of the dynamic scan series for interleaved acquisitions of T_2* maps and ^{31}P-MRS during plantar flexion exercise and subsequent recovery. The effective TR for both readouts was 3 seconds, yielding a temporal resolution of 3 seconds for ^{31}P-MR spectra and ^{1}H MRI of the BOLD response. Tissue concentrations of ATP, PCr, and P_i as well as the tissue pH are plotted against time, revealing PCr depletion during exercise and subsequent recovery after cessation of exercise. Median normalized gastrocnemius (G) and soleus (S) muscle R_2* values were determined from ROIs in the T_2* maps, and plotted against time to characterize the BOLD response to exercise. Time courses of the PCr and P_i concentrations are included in the graph for a direct comparison of tissue oxygenation dynamics with high-energy phosphate metabolism during the same exercise-recovery protocol. T_2* maps acquired during exercise were discarded due to motion artifacts. ATP, adenosine 5′-triphosphate; BOLD, blood oxygenation level-dependent; PCr, phosphocreatine; P_i, inorganic phosphate.

None of the patients complained of symptomatic pain after performing in-magnet plantar flexion exercise. Datasets from three healthy subjects were excluded due to a mechanical failure of the exercise device or poor data quality due to motion during the recovery phase. Datasets from two patients were excluded from the analyses due to insufficient adherence to the exercise protocol. Participant characteristics (n = 15 healthy subjects; n = 13 patients) are listed in Table 1. Age and BMI were comparable for patients and healthy control subjects. The ABI in patients was lower compared with healthy subjects

(0.71 ± 0.24 vs. 1.25 ± 0.17; $P < 0.001$). Low-density lipoprotein (LDL) cholesterol levels were lower in PAD patients compared with healthy subjects (2.50 ± 0.82 vs. 3.43 ± 0.79 mM; $P < 0.01$), with a concomitantly lower total cholesterol level in PAD patients (4.48 ± 1.10 vs. 5.46 ± 0.90 mM; $P < 0.05$). Other blood measures were similar for patients and healthy control subjects.

We obtained T_2* maps of the calf musculature to assess tissue oxygenation dynamics via the BOLD response to plantar flexion exercise. Mean normalized R_2* time curves are

TABLE 1. General Characteristics and Blood Panel Results of Study Participants

	Healthy control subjects ($n = 15$)	Peripheral artery disease patients ($n = 13$)
Gender (male/female)	8/7	7/6
Age (y)	58.0 ± 8.7	59.7 ± 7.3
BMI (kg/m^2)	24.6 ± 3.5	27.5 ± 5.2
Systolic blood pressure (mmHg)	133 ± 26	140 ± 23
Diastolic blood pressure (mmHg)	85 ± 9.1	80 ± 9.4
ABI (–)	1.25 ± 0.17	0.71 ± 0.24***
Blood panel results		
hemoglobin (mM)	8.85 ± 0.77	9.18 ± 0.98
hematocrit (L/L)	0.43 ± 0.031	0.44 ± 0.053
platelets (×10^9/L)	242 ± 58	269 ± 85
MCV (fL)	90.1 ± 4.1	92.4 ± 4.1
WBC count (×10^9/L)	6.41 ± 1.22	7.64 ± 2.59
total cholesterol (mM)	5.46 ± 0.90	4.48 ± 1.10*
HDL cholesterol (mM)	1.55 ± 0.47	1.27 ± 0.40
LDL cholesterol (mM)	3.43 ± 0.79	2.50 ± 0.82**
triglycerides (mM)	1.09 ± 0.49	1.53 ± 1.24
creatinine (μM)	76.6 ± 16.2	81.6 ± 23.1
glucose (mM)	5.60 ± 1.13	5.53 ± 0.40

ABI, ankle-brachial index; BMI, body-mass index; HDL, high-density lipoprotein; LDL, low-density lipoprotein; MCV, mean corpuscular volume; WBC, white blood cells.
*$P < 0.05$; **$P < 0.01$; ***$P < 0.0001$ vs. healthy control subjects (two-sided Mann–Whitney U-test).

displayed in Fig. 2a,b, and derived parameters are summarized in Table 2. Gastrocnemius and soleus R_2* at end-recovery were similar, showed a strong correlation ($r = 0.82$; $P < 0.0001$), and did not differ between patients and healthy subjects. In the gastrocnemius muscle for 8 out of 13 PAD patients and for 7 out of 15 healthy subjects, tissue hyperemia during recovery was observed in the R_2* time curves. The relative amplitude of this BOLD response was higher in PAD patients compared with healthy subjects (–3.8 ± 1.4% vs. –1.4 ± 0.3%; $P < 0.001$), and showed a strong correlation with the ABI for both groups combined ($r = 0.79$; $P < 0.001$; Fig. 2c). The associated time-to-peak was similar for both groups. Any hyperemic BOLD responses in soleus muscle were not different between groups.

Good-quality ^{31}P-MR spectra were obtained throughout the exercise-recovery protocol (Fig. 3a). Parameters of calf muscle high-energy phosphate metabolism are reported in Table 3. Resting-state PCr, P$_i$, PDE, and ADP concentrations and tissue pH were similar for patients and healthy subjects. PCr depletion in the calf muscle by plantar flexion exercise was somewhat higher in patients than in healthy subjects (36.1 ± 11.9% vs. 27.6 ± 7.9%; $P < 0.05$). End-exercise PDE concentration was lower for PAD patients compared with healthy subjects (3.2 ± 1.5 vs. 4.8 ± 1.4 mM; $P < 0.01$), whereas PCr, P$_i$, and ADP concentrations as well as pH were not different between groups. End-exercise pH showed a strong negative correlation with PCr depletion in healthy subjects ($r = -0.83$; $P < 0.001$), but not in PAD patients. Moreover, end-exercise pH was similar to resting-state pH, and remained well above the level of acidosis in all participants.[26] The PCr recovery time constant τ_{PCr} ($r^2 = 0.88 ± 0.077$) was much higher for patients than for healthy subjects (52.0 ± 13.5 vs. 30.3 ± 9.7 s; $P < 0.0001$). Moreover, τ_{PCr} showed a strong negative correlation with the ABI for both groups combined ($r = -0.64$; $P < 0.001$; Fig. 3b).

The interleaved acquisitions of T$_2$* maps and ^{31}P-MR spectra allowed us to make a direct comparison of the BOLD response and PCr recovery kinetics under identical
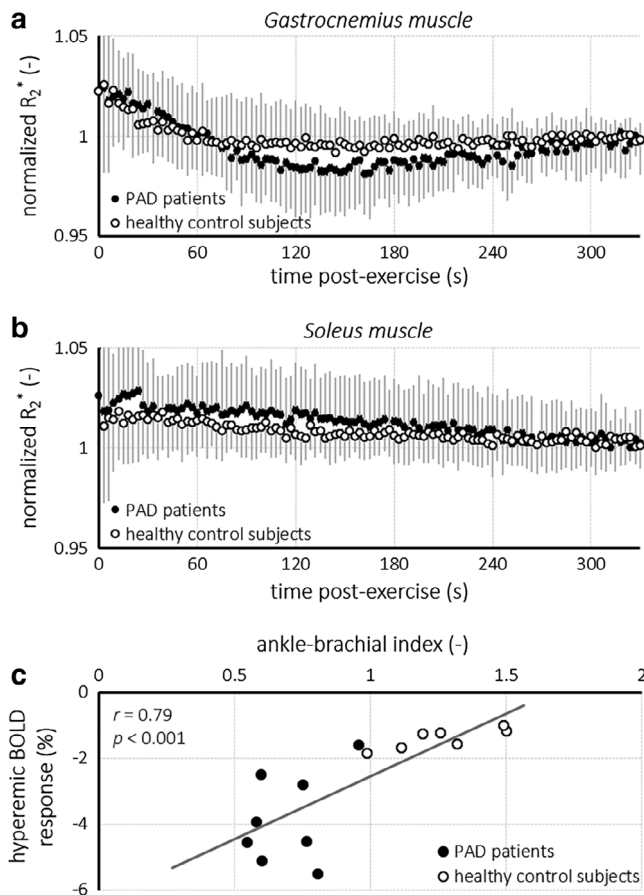
FIGURE 2: Time curves of the normalized R_2* for the gastrocnemius muscle (a) and soleus muscle (b) for PAD patients (shaded circles) and healthy control subjects (open circles) obtained during recovery after plantar flexion exercise. The amplitude of the hyperemic BOLD response in the gastrocnemius muscle correlated ($r = 0.79$; $P < 0.001$) with the ABI for PAD severity (c). BOLD, blood oxygenation level-dependent.

performance in PAD. In this study we used interleaved acquisitions of ^{1}H T_2* maps and ^{31}P-MR spectra to measure the BOLD response and PCr recovery kinetics essentially simultaneously during a single exercise-recovery session in PAD patients and healthy control subjects. Using this multinuclear approach, we found evidence to support disturbed energy metabolism and altered tissue oxygenation dynamics in calf muscles of PAD patients. Particularly, PCr recovery after exercise was delayed in PAD, which was associated with functional hyperemia in the gastrocnemius muscle. Both measures correlated strongly with the clinical measure of PAD severity, the ABI, demonstrating that our noninvasive measurements can provide a quantitative window on calf muscle pathophysiology in PAD.

The higher PCr recovery time constant τ_{PCr} in PAD patients compared with healthy subjects suggests a reduced mitochondrial oxidative capacity in calf skeletal muscle of PAD patients.[8] Several studies that utilized ^{31}P-MRS to measure PCr recovery kinetics after in-magnet plantar flexion exercise have been reported for PAD patients,[9–12,15,29] all showing that PCr recovery is prolonged in PAD. Our data are consistent with these prior studies, although the τ_{PCr} for PAD found here (52.0 ± 13.5 sec; highest 75.5 sec) is somewhat low compared with some other studies that report time constants of >100 sec for some subjects[10–12,15] with similar PAD severity (Fontaine stage II). Our exercise protocol was relatively mild, with a PCr depletion of ~30% compared with previous work that exceeded 50% PCr depletion.[11,12] Importantly, in contrast to previous studies,[11,15] the modest PCr depletion in the current protocol did not induce tissue acidosis in any of the participants, which otherwise would have slowed down PCr recovery.[26] The pronounced difference in τ_{PCr} between PAD patients and healthy control subjects suggests that ^{31}P-MRS during an exercise-recovery protocol may aid in establishing PAD severity by quantifying skeletal muscle performance. It also provides a potentially useful noninvasive method to monitor efficacy of treatment strategies.[9,10]

Previous studies evaluating ^{31}P-MRS readouts of high-energy phosphate metabolism with tissue perfusion or oxygenation measures obtained with MR[15] or with near-infrared spectroscopy (NIRS) and Doppler ultrasound[12] required two exercise sessions on separate days. Notably, those studies did not report any correlations between PCr recovery kinetics and tissue perfusion[15] or oxygenation.[12] In contrast, a study that combined ^{31}P-MRS and NIRS during a single exercise-recovery protocol reported a strong correlation between simultaneously measured PCr recovery and tissue reoxygenation time constants.[29] Here, by combining BOLD MRI and ^{31}P-MRS, we also established a correlation between alterations in high-energy phosphate metabolism and tissue oxygenation dynamics in PAD patients compared with healthy control subjects, emphasizing the added value of such simultaneous assessments of muscle tissue physiology.

physiological conditions of a single exercise-recovery experiment. Notably, PCr recovery after exercise was slower in those subjects with a stronger hyperemic effect in the gastrocnemius muscle, evidenced by a strong negative correlation of τ_{PCr} with the amplitude of the hyperemic BOLD response in the gastrocnemius muscle R_2* values ($r = -0.66$; $P < 0.01$; Fig. 4a), but not in the soleus muscle. Similarly, PCr depletion ($r = -0.72$; $P < 0.01$) and concomitantly the end-exercise P_i concentration ($r = -0.69$; $P < 0.01$; Fig. 4b), but not end-exercise pH, correlated negatively with the gastrocnemius muscle BOLD response amplitude during hyperemia. In contrast, no correlations between any readouts of ^{31}P-MRS with BOLD MRI of the soleus muscle existed.

Discussion

Both impaired skeletal muscle tissue oxygenation and perfusion[12,27] as well as intrinsic mitochondrial dysfunction[28] have been implicated in the pathophysiology of decreased muscle

TABLE 2. Calf Muscle Metrics From Dynamic Blood Oxygenation Level-Dependent MRI After Exercise in Healthy Control Subjects and Peripheral Artery Disease Patients

	Healthy control subjects ($n = 15$)	Peripheral artery disease patients ($n = 13$)
Gastrocnemius muscle		
end-exercise deoxygenation (%)	1.9 ± 2.6	2.2 ± 2.1
hyperemia (n) [%]	7/15 [47%]	8/13 [62%]
amplitude (%)	-1.4 ± 0.3	-3.8 ± 1.4***
time-to-peak (s)	186 ± 80	128 ± 30
end-recovery R_2* (s^{-1})	0.045 ± 0.007	0.042 ± 0.005
Soleus muscle		
end-exercise deoxygenation (%)	1.5 ± 2.4	2.3 ± 2.9
hyperemia (n)	7/15 [47%]	5/13 [38%]
amplitude (%)	-2.2 ± 1.3	-1.6 ± 0.2
time-to-peak (s)	250 ± 139	189 ± 114
end-recovery R_2* (s^{-1})	0.045 ± 0.008	0.044 ± 0.004

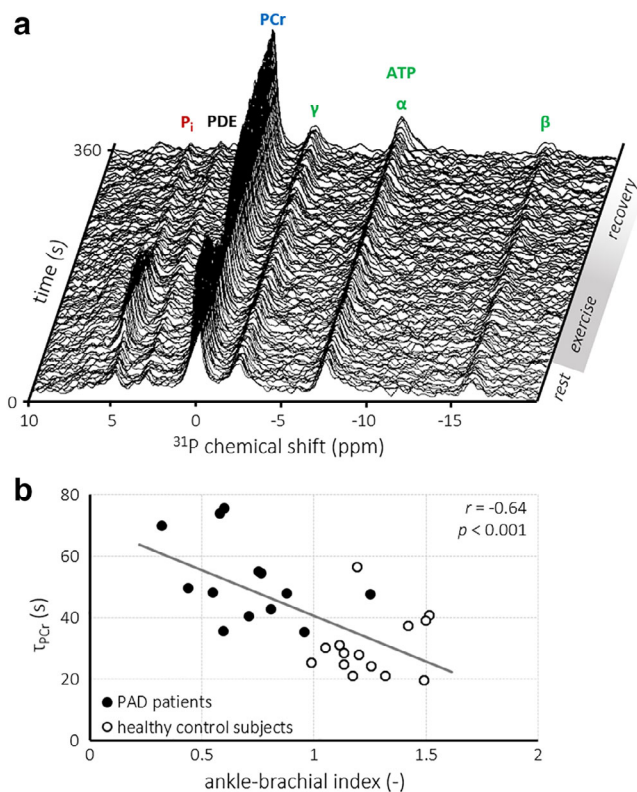***$P < 0.001$ vs. healthy control subjects (two-sided Mann–Whitney U-test).

FIGURE 3: Series of ^{31}P-MR spectra obtained during plantar flexion exercise and subsequent recovery in a healthy control subject (a). The PCr recovery time constant (τ_{PCr}) showed a strong negative correlation ($r = -0.64$; $P < 0.001$) with the ABI for PAD severity (b). ATP, adenosine 5′-triphosphate; PDE, phosphodiesters; P_i, inorganic phosphate.

Thus far, BOLD MRI has predominantly been employed to assess reactive hyperemia in an ischemia–reperfusion paradigm, or to measure transient effects after single short-term muscle contractions.[30] We observed functional hyperemia in the BOLD response after exercise for at least a subset of participants in the present study. Our data are in line with some previous results that used either radioactive tracers,[31] NIRS,[32] T_2*-weighted MRI,[14] dynamic contrast-enhanced ultrasound imaging,[33] or dynamic contrast-enhanced MRI[34] to demonstrate calf muscle hyperemia during recovery after exercise in PAD patients. The functional hyperemia and its higher amplitude we observed in the gastrocnemius muscle of most PAD patients may be indicative of elevated levels of hypoxic metabolic end products that trigger a vasodilatory blood flow adaptation during recovery from exercise-induced tissue deoxygenation.[33] In apparent contrast, reactive hyperemia after cuff-induced occlusion and subsequent reperfusion was shown to be blunted in PAD patients compared with healthy control subjects.[13,27,33] Although an ischemia–reperfusion paradigm allows for a well-controlled stimulus that provokes a response at the maximally available vascular capacity, exercise is more relevant to the pathophysiology of intermittent claudication in PAD.[35] With mild exercise that did not lead to claudication pain, we were able to detect differences in the gastrocnemius muscle BOLD response between healthy subjects and PAD patients that related to PAD severity. The absence of correlations of any ^{31}P-MRS readouts with the BOLD response in the soleus muscle is consistent with the notion that the gastrocnemius muscle

	Healthy control subjects (n = 15)	Peripheral artery disease patients (n = 13)
TABLE 3. Calf Muscle High-Energy Phosphate Metabolism Parameters Measured With ^{31}P-MRS at Rest and After Exercise in Healthy Control Subjects and Peripheral Artery Disease Patients		
PCr (mM)		
rest	34.6 ± 2.6	35.5 ± 3.2
end-exercise	25.1 ± 3.7	23.9 ± 5.7
PCr depletion (%)	27.6 ± 7.9	36.1 ± 11.9*
τ_{PCr} (s)	30.3 ± 9.7	52.0 ± 13.5***
P_i (mM)		
rest	5.1 ± 1.1	6.0 ± 1.6
end-exercise	13.2 ± 2.7	16.0 ± 4.1
PDE (mM)		
rest	5.4 ± 1.5	4.6 ± 0.8
end-exercise	4.8 ± 1.4	3.2 ± 1.5**
ADP (mM)		
rest	10.3 ± 0.9	10.3 ± 1.2
end-exercise	35.4 ± 7.6	47.6 ± 29.6
pH (–)		
rest	7.06 ± 0.03	7.07 ± 0.05
end-exercise	7.05 ± 0.05	7.06 ± 0.04

ADP, adenosine diphosphate; PCr, phosphocreatine; PDE, phosphodiesters; P_i, inorganic phosphate; τ_{PCr}, PCr recovery time constant.
*$P < 0.05$; **$P < 0.01$; ***$P < 0.0001$ vs. healthy control subjects (two-sided Mann–Whitney U-test).

FIGURE 4: Correlations between the relative amplitude of the hyperemic BOLD response in the gastrocnemius muscle and the PCr recovery time constant (τ_{PCr}) (a) and the end-exercise inorganic phosphate (P_i) concentration (b), acquired during the same exercise-recovery session. BOLD, blood oxygenation level-dependent; P_i, inorganic phosphate.

is more active than the soleus muscle during plantar flexion with a fully extended knee.[34,36]

There are some limitations in the current study. The sample size was relatively small and included PAD patients at Fontaine stage II only. Yet the muscle BOLD responses after exercise, and particularly hyperemic effects, if any, were rather heterogeneous. Indeed, a previous study showed that repeatability of BOLD MRI at 1.5T is poor for calf musculature in PAD patients and healthy volunteers during reactive hyperemia after cuff-induced occlusion,[37] which was attributed to large physiological day-to-day variations. Differences in peripheral vascular anatomy may also contribute to the heterogeneity we observed here. Furthermore, we note that measurements during plantar flexion were conducted in the supine position, which may
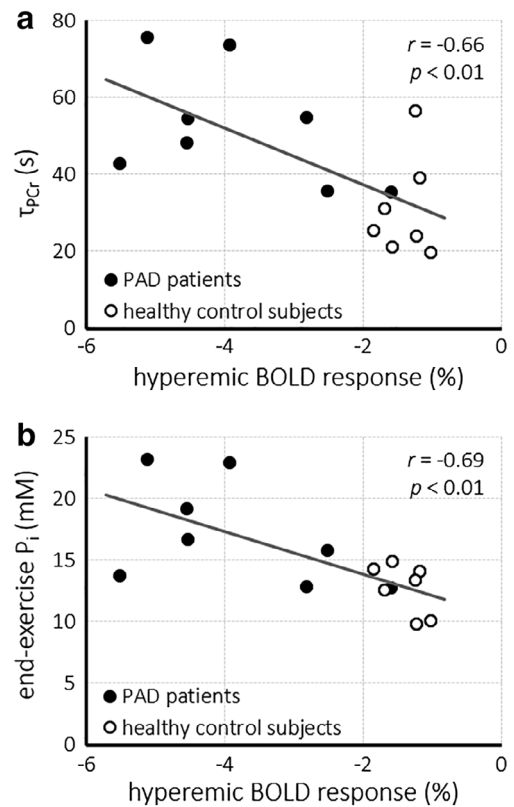
mitigate some of the vascular impairments experienced when standing upright. Our approach of interleaved acquisitions allowed for a direct comparison of surrogate measures of tissue oxygenation with readouts of high-energy phosphate metabolism during the same exercise-recovery session. Prospective studies in a large cohort of asymptomatic subjects are needed to investigate the prognostic value of the proposed method, and to substantiate the correlations we found here. A quantitative comparison of patients before and after a therapeutic intervention, such as revascularization or vasodilatory medication with cilostazol, will be instrumental to demonstrate any added value of this approach for treatment monitoring. We anticipate that with ongoing developments in MR hardware such as dual-frequency ^{1}H/^{31}P coil arrays,[38] acquisition schemes[17] and sequences,[39] and the emerging use of 7T MR systems,[36,40] the sensitivity of BOLD MRI and ^{31}P-MRS to dynamic changes and pathophysiologic alterations as well as the spatial coverage of the calf musculature will increase. In addition, simultaneous readouts of tissue high-energy phosphate metabolism with ^{31}P-MRS and measures obtained with ^{1}H-MRI will be of benefit for studies of other organs including the brain and the heart, such that any correlations between different physiological parameters can truly be obtained during the same challenge or stimulus as we demonstrated here.

In conclusion, we demonstrated the feasibility of an essentially simultaneous multinuclear MR assessment of calf muscle tissue oxygenation and high-energy phosphate metabolism during a single exercise-recovery session. The functional hyperemic BOLD response to exercise in the gastrocnemius muscle correlated with the PCr recovery time constant, showing that any pronounced hypoxia-triggered vasodilation in PAD is associated with a reduced mitochondrial oxidative capacity. Interleaving BOLD MRI and ^{31}P-MRS thus allows for a dynamic assessment of skeletal muscle (patho)physiology in response to exercise. Such multiparametric MR readouts will be clinically relevant in the noninvasive longitudinal testing of therapeutic interventions that aim at improving microvascular and muscular function in PAD.

Acknowledgments

References

1. Bhatt DL, Steg PG, Ohman EM, et al. International prevalence, recognition, and treatment of cardiovascular risk factors in outpatients with atherothrombosis. JAMA 2006;295:180–189.

2. Fowkes FGR, Rudan D, Rudan I, et al. Comparison of global estimates of prevalence and risk factors for peripheral artery disease in 2000 and 2010: A systematic review and analysis. Lancet 2013;382:1329–1340.

3. Wennberg PW. Approach to the patient with peripheral arterial disease. Circulation 2013;128:2241–2250.

4. Aboyans V, Criqui MH, Abraham P, et al. Measurement and interpretation of the ankle-brachial index. Circulation 2012;126:2890–2909.

5. de Graaff JC, Ubbink DT, Legemate DA, Tijssen JG, Jacobs MJH. Evaluation of toe pressure and transcutaneous oxygen measurements in management of chronic critical leg ischemia: A diagnostic randomized clinical trial. J Vasc Surg 2003;38:528–534.

6. Carlier PG, Marty B, Scheidegger O, et al. Skeletal muscle quantitative nuclear magnetic resonance imaging and spectroscopy as an outcome measure for clinical trials. J Neuromuscul Dis 2016;3:1–28.

7. Mathew RC, Kramer CM. Recent advances in magnetic resonance imaging for peripheral artery disease. Vasc Med 2018;23:143–152.

8. Lanza IR, Bhagra S, Nair KS, Port JD. Measurement of human skeletal muscle oxidative capacity by ^{31}P-MR spectroscopy: A cross-validation with in vitro measurements. J Magn Reson Imaging 2011;34:1143–1150.

9. Hands LJ, Bore PJ, Galloway G, Morris PJ, Radda GK. Muscle metabolism in patients with peripheral vascular disease investigated by ^{31}P nuclear magnetic resonance spectroscopy. Clin Sci (Lond) 1986;71:90–283.

10. Isbell DC, Berr SS, Toledano AY, et al. Delayed calf muscle phosphocreatine recovery after exercise identifies peripheral arterial disease. J Am Coll Cardiol 2006;47:2289–2295.

11. Greiner A, Esterhammer R, Messner H, et al. High-energy phosphate metabolism during incremental calf exercise in patients with unilaterally symptomatic peripheral arterial disease measured by phosphor-31 magnetic resonance spectroscopy. J Vasc Surg 2006;43:978–986.

12. Hart CR, Layec G, Trinity JD, et al. Oxygen availability and skeletal muscle oxidative capacity in patients with peripheral artery disease: Implications from in vivo and in vitro assessments. Am J Physiol Circ Physiol 2018;315:H897–H909.

13. Ledermann H-P, Schulte A-C, Heidecker H-G, et al. Blood oxygenation level-dependent magnetic resonance imaging of the skeletal muscle in patients with peripheral arterial occlusive disease. Circulation 2006; 113:2929–2935.

14. Li Z, Muller MD, Wang J, et al. Dynamic characteristics of T_2*-weighted signal in calf muscles of peripheral artery disease during low-intensity exercise. J Magn Reson Imaging 2017;46:40–48.

15. Anderson JD, Epstein FH, Meyer CH, et al. Multifactorial determinants of functional capacity in peripheral arterial disease: Uncoupling of calf muscle perfusion and metabolism. J Am Coll Cardiol 2009;54:628–635.

16. Meyerspeer M, Kemp GJ, Mlynárik V, et al. Direct noninvasive quantification of lactate and high energy phosphates simultaneously in exercising human skeletal muscle by localized magnetic resonance spectroscopy. Magn Reson Med 2007;57:60–654.

17. Wary C, Nadaj-Pakleza A, Laforêt P, et al. Investigating glycogenosis type III patients with multi-parametric functional NMR imaging and spectroscopy. Neuromuscul Disord 2010;20:548–558.

18. Hardman R, Jazaeri O, Yi J, Smith M, Gupta R. Overview of classification systems in peripheral artery disease. Semin Intervent Radiol 2014; 31:378–388.

19. Henningsson M, Mens G, Koken P, Smink J, Botnar RM. A new framework for interleaved scanning in cardiovascular MR: Application to image-based respiratory motion correction in coronary MR angiography. Magn Reson Med 2015;73:692–696.

20. Klein S, Staring M, Murphy K, Viergever MA, Pluim J. elastix: A toolbox for intensity-based medical image registration. IEEE Trans Med Imaging 2010;29:196–205.

21. Vanhamme L, van den Boogaart A, Van Huffel S. Improved method for accurate and efficient quantification of MRS data with use of prior knowledge. J Magn Reson 1997;129:35–43.

22. Kemp GJ, Meyerspeer M, Moser E. Absolute quantification of phosphorus metabolite concentrations in human muscle in vivo by ^{31}P MRS: A quantitative review. NMR Biomed 2007;20:555–565.

23. Taylor DJ, Bore PJ, Styles P, Gadian DG, Radda GK. Bioenergetics of intact human muscle: A ^{31}P nuclear magnetic resonance study. Mol Biol Med 1983;1:77–94.

24. Lawson JW, Veech RL. Effects of pH and free Mg_2+ on the K_{eq} of the creatine kinase reaction and other phosphate hydrolyses and phosphate transfer reactions. J Biol Chem 1979;254:37–6528.

25. Boska M. ATP production rates as a function of force level in the human gastrocnemius/soleus using ^{31}P MRS. Magn Reson Med 1994; 32:1–10.

26. van den Broek NMA, De Feyter HMML, de Graaf L, Nicolay K, Prompers JJ. Intersubject differences in the effect of acidosis on phosphocreatine recovery kinetics in muscle after exercise are due to differences in proton efflux rates. Am J Physiol Physiol 2007;293: C228–C237.

27. Englund EK, Langham MC, Ratcliffe SJ, et al. Multiparametric assessment of vascular function in peripheral artery disease. Circ Cardiovasc Imaging 2015;8:e002673.

28. Pipinos II, Judge AR, Selsby JT, et al. The myopathy of peripheral arterial occlusive disease: Part 1. Functional and histomorphological changes and evidence for mitochondrial dysfunction. Vasc Endovascular Surg 2008;41:481–489.

29. Kemp GJ, Roberts N, Bimson WE, et al. Mitochondrial function and oxygen supply in normal and in chronically ischemic muscle: A combined ^{31}P magnetic resonance spectroscopy and near infrared spectroscopy study in vivo. J Vasc Surg 2001;34:1103–1110.

30. Jacobi B, Bongartz G, Partovi S, et al. Skeletal muscle BOLD MRI: From underlying physiological concepts to its usefulness in clinical conditions. J Magn Reson Imaging 2012;35:1253–1265.

31. Alpert JS, Larsen OA, Lassen NA. Exercise and intermittent claudication: Blood flow in the calf muscle during walking studied by the xenon-133 clearance method. Circulation 1969;39:353–359.

32. Kooijman HM, Hopman MTE, Colier WNJM, van der Vliet JA, Oeseburg B. Near infrared spectroscopy for noninvasive assessment of claudication. J Surg Res 1997;72:1–7.

33. Meneses AL, Nam MCY, Bailey TG, et al. Leg blood flow and skeletal muscle microvascular perfusion responses to submaximal exercise in peripheral arterial disease. Am J Physiol Circ Physiol 2018;315:H1425–H1433.

34. Zhang JL, Layec G, Hanrahan C, et al. Exercise-induced calf muscle hyperemia: Quantitative mapping with low-dose dynamic contrast enhanced magnetic resonance imaging. Am J Physiol Circ Physiol 2019;316:H201–H211.

35. Lopez D, Pollak AW, Meyer CH, et al. Arterial spin labeling perfusion cardiovascular magnetic resonance of the calf in peripheral arterial disease: Cuff occlusion hyperemia vs exercise. J Cardiovasc Magn Reson 2015;17:23.

36. Niess F, Fiedler GB, Schmid AI, et al. Dynamic multivoxel-localized ^{31}P MRS during plantar flexion exercise with variable knee angle. NMR Biomed 2018;31:e3905.

37. Versluis B, Backes WH, van Eupen MGA, et al. Magnetic resonance imaging in peripheral arterial disease: Reproducibility of the assessment of morphological and functional vascular status. Invest Radiol 2011;46:11–24.

38. Goluch S, Kuehne A, Meyerspeer M, et al. A form-fitted three channel ^{31}P, two channel ^{1}H transceiver coil array for calf muscle studies at 7 T. Magn Reson Med 2015;73:2376–2389.

39. Santos-Díaz A, Harasym D, Noseworthy MD. Dynamic ^{31}P spectroscopic imaging of skeletal muscles combining flyback echo-planar spectroscopic imaging and compressed sensing. Magn Reson Med 2019;81:3453–3461.

40. Towse TF, Childs BT, Sabin SA, Bush EC, Elder CP, Damon BM. Comparison of muscle BOLD responses to arterial occlusion at 3 and 7 Tesla. Magn Reson Med 2016;75:1333–1340.